

# Modeling Human-AI Team Decision Making

Wei Ye,<sup>1</sup> Francesco Bullo,<sup>2</sup> Noah Friedkin,<sup>2</sup> Ambuj K Singh<sup>2\*</sup>

<sup>1</sup> Tongji University, Shanghai 201804, China

<sup>2</sup> University of California, Santa Barbara, CA 93106, USA  
ambuj@cs.ucsb.edu

## Abstract

AI and humans bring complementary skills to group deliberations. Modeling this group decision making is especially challenging when the deliberations include an element of risk and an exploration-exploitation process of appraising the capabilities of the human and AI agents. To investigate this question, we presented a sequence of intellectual issues to a set of human groups aided by imperfect AI agents. A group's goal was to appraise the relative expertise of the group's members and its available AI agents, evaluate the risks associated with different actions, and maximize the overall reward by reaching consensus. We propose and empirically validate models of human-AI team decision making under such uncertain circumstances, and show the value of socio-cognitive constructs of prospect theory, influence dynamics, and Bayesian learning in predicting the behavior of human-AI groups.

## 1 Introduction

Group decision making has been ever important in organizations and missions. And now, intelligent agents have become fundamental to everyday life: assistants on mobile devices, pedagogical agents in tutoring systems, and robots collaborating with humans. As such, integrating AI agents into human groups while being aware of their complementary strengths and abilities has become vital (Crandall et al. 2018; Gaur et al. 2016; Kamar, Hacker, and Horvitz 2012; Shirado and Christakis 2017; Wang et al. 2016). We explore models for decision making in mixed teams while building on the constructs of prospect theory and appraisal systems.

Groups/teams frequently encounter decisions involving varying amounts of risk and reward. Cumulative Prospect Theory (Tversky and Kahneman 1992a) (formerly Prospect Theory (Kahneman and Tversky 1979a)) provides a basis for such decision-making by establishing that individuals make decisions based on the potential value of losses and gains among the set of available options. Cumulative Prospect Theory proposes that individuals compute an internal evaluation for each prospect that is determined by a value function and a probability weighting function. The value function is S-shaped and asymmetrical, capturing loss aversion. The

probability weighting function encodes the hypothesis that individuals overreact to small probability events, but under-react to large probability events.

Group decision making is based on how team members appraise others. Team members' opinions of others depend on the issue and evolve over time, based on their performance. Such opinions can be represented by an appraisal network (Mei et al. 2017), or equivalently by its corresponding row-stochastic appraisal matrix. The edges of this matrix are weighted, depict trust/distrust, friendship/animosity, or more generally to what degree a team member is influenced by particular others. The eigenvector centrality of each person in an irreducible aperiodic appraisal matrix is a summary measure of each team member's relative importance in determining the team's decision making.

In order to understand how a human-AI team reaches a decision in uncertain environments, we carried out cyber-human experiments in which a team is asked to answer a sequence of questions. The task is to answer intellectual questions from different categories such as history, science and technology, etc. Every team consists of four members each with access to its own AI agent. The AI agents give the correct answer at a fixed probability (unknown to the team members); however, the baseline probabilities vary across the agents. Each question is answered in four timed phases. In the first phase, every team member records his/her individual response for the question. In the second phase, the response of every team member is displayed on the screen and a chat plugin (the only communication channel) is enabled for communication. Team members then record their choices and decide whether or not to use an AI agent (and which AI agent to use) in an optional third phase. In the fourth and final phase, the team submits an answer. The correct answer to each question is displayed at the end of each round. Note that if the group has relied on the incorrect response of an AI agent, then the group's trust in that agent (and their other available AI agents) may be eroded. After every five questions an influence survey is presented. This is filled in by each team member to record the relative direct influence of each of his/her teammates on his/her opinion. The team members are also asked to rate the accuracy of all four AI agents based on their interactions with them.

The first step of a team's decision making consists of deliberating and choosing one of the multiple choice options

\*To whom correspondence should be addressed.

or choosing to consult an AI agent. In case a team chooses to consult an AI agent, the second decision making step consists of integrating the agent's answer with the team's choices and reporting a final answer. Each possible action in a decision making step is associated with a probability of success and a reward. From the viewpoint of Prospect Theory, each action is a gamble and the team needs to choose between multiple gambles. We observe the actions by the teams but not the perceived probability of success, probability weighting function, or the valuation function.

We investigate and compare four models that predict the decisions of the teams. The first two models capture the appraisal process in a team, while the last two models capture the appraisal process as well as decision making under risks. We outline these four models below.

The first model, **NB** (Naive Bayes), captures the accuracy of a human/AI-agent using a beta distribution that is updated at each round (after observing whether it was correct or incorrect) using Bayes rule. A Naive Bayes assumption is used to integrate the responses of the human/AI-agents and obtain the probability of using an option or an agent. The second model, **CENT** (Centrality), integrates individual responses through an interpersonal influence system. The probability of the team choosing an option is computed as the sum of the eigenvector centrality values of each individual choosing that option. The assumption underlying this computation is always satisfied in our data. A similar weighting process is used to integrate the team's evaluation of the AI-agents. The third model, **PT-NB** (Prospect Theory coupled with Naive Bayes), uses Prospect Theory to analyze the actions of the team as a set of gambles. The probabilities of success and reward of each gamble are computed as in the model **NB**. The team chooses among these gambles based on Prospect Theory parameters of the team (learned through an initial training sequence). The final model, **PT-CENT** (Prospect Theory coupled with Centrality), again uses Prospect Theory to analyze the actions of the team as a set of gambles. The probabilities of success and reward of each gamble are computed as in the model **CENT**. A team again chooses among these gambles based on Prospect Theory.

We measure the accuracy of the above four models using our experimental data. This measurement is non-trivial since only the team's chosen action is observed and not the team's detailed preferences for each of the actions. We resolve this difficulty by considering the set of probability distributions (on the actions) over which the chosen action is dominant and computing the minimum distance (based on cross-entropy loss) over this set to the model's predicted probability distribution.

## 2 Related Work

Group performance is not simply a sum of individual performance, but ruled by patterns of interactions, influence, and other relationships among group members. We know that transactive memory systems (TMS) (Wegner 1987)) are activated in group members' levels of expertise and potential contributions to tasks are appraised. We know that interpersonal influence systems are automatically generated in groups (Friedkin and Johnsen 2011). And we know that

groups' opinions on multidimensional issues are generally constrained to a decision space of feasible positions that is the group's convex hull of initial displayed positions (Friedkin et al. 2019).

An excellent survey of human-AI teaming has been put forth in a recent paper (O'Neill et al. 2020). (DeCostanza et al. 2018) discusses the mechanisms for enhancing teamwork in human-AI teams and outlines the critical scientific questions that must be addressed to enable this vision.

Group constructs have also been proposed in machine learning—experts, weak learners, crowd-sourced workers—to achieve goals that no single individual can accomplish on its own. In the case of boosting (Schapire 1990), one can obtain a “strong learner” that is able to predict arbitrarily accurately based on an ensemble of “weak learners” whose predictions are slightly better than random guessing. In the case of “learning from expert advice” (Cesa-Bianchi et al. 1997), an algorithm works with a group of  $K$  arbitrary “experts” who give daily “stock predictions” and who perform nearly as well as the “expert” that has the best “track record” at any given time. It is an iterative game in which in each iteration the “player” must make a decision and the experts with the best track record may change over time. The “Multi-armed Bandits” (MAB) problems (Auer, Cesa-Bianchi, and Fischer 2002) can be thought of as a variant of the problem of “learning from expert advice” in which a “player” can only observe the payoff of the “expert” at each iteration. In the case of “crowd sourcing” (Welinder et al. 2010), an algorithm aggregates the inputs of a large group of unreliable “participants”, evaluates each “participant”, and then infers the ground truth.

Humans and AI are clearly different in their cognitive and processing capabilities (Cummings 2014). Groups with AI involvement should be designed so that the raw computational and search power of computers for state-space reduction can be combined with group inductive reasoning, especially in uncertain environments. What is the optimal group-AI design for a given decision? This is a question pervading all kinds of groups that oriented to specific types of issues. Taxonomies and ontologies for characterizing group decision-making have been defined (Sheridan and Verplank 1978; Endsley and Kaber 1999; Rasmussen 1987) in order to investigate the optimal composition of groups. The behavior of groups with AI involvement must be observable and predictable. This is challenging in complex uncertain environments. While groups often adopt satisficing strategies (Simon 1957; Friedkin et al. 2019), AI utilizes search space reduction strategies such as limited look-ahead, constraint relaxation, and heuristics. Both groups and AI are subject to bias and faulty information: groups by their members' beliefs and AI by the available data and training protocols. Since observability and predictability have ramifications on the level of trust (Stubbs, Hinds, and Wettergreen 2007), groups with AI involvement must have confidence that the behavior of their AI is consistent with an acceptable common ground whatever the displayed initial beliefs of the group's members might be (Marathe et al. 2018b; Li, Sun, and Miller 2016; Chen and Barnes 2014; Telesford et al. 2016; Garcia et al. 2017; Marathe et al. 2018a).

Theory of mind (ToM) (Premack and Woodruff 1978; Baker, Saxe, and Tenenbaum 2011; Cuzzolin et al. 2020; Oguntola, Hughes, and Sycara 2021; Rabinowitz et al. 2018) broadly refers to humans’ ability to represent the mental states of others, including their desires, beliefs, and intentions. This ability to attribute mental states to others is a key component of cognition that needs to be incorporated into AI in order to model and interact with humans.

Human teams can display magnified cognitive capacity and unique cognitive abilities that emerge from the interaction between the team members. Collective intelligence refers to a team’s ability to produce intelligence and behaviors beyond the individual (Woolley et al. 2010). How to integrate AI into human teams in order to produce cognitive abilities that go beyond the individual or the group of humans is an important question (Bansal et al. 2019).

Research from psychology suggests that people process uncertainty and information in general using dual processes: an implicit (automatic), unconscious process and an explicit (controlled), conscious process (Chaiken and Trope 1999). The second process is encoded by analytic algorithms, rules, and reasoning systems, and can be modeled equally well for humans and AI agents. It is the first implicit automatic system and its interaction with the explicit system that is harder to model in humans, and poses challenges for a theoretical understanding of mixed human-AI teams.

Uncertainty itself can be separated into two kinds: aleatoric and epistemic (Der Kiureghian and Ditlevsen 2009; Fox and Ülkümen 2011). Aleatoric uncertainty refers to the notion of randomness (as in coin flipping): the variability in the outcome of an experiment that is due to inherently random effects. Epistemic uncertainty refers to uncertainty caused by a lack of knowledge of decision makers. This uncertainty can in principle be reduced by a proper recognition of expertise on teams and protocols that reveal explanations on why a fact may be true.

Both aleatoric and epistemic uncertainty require teams to deal with decisions involving varying amounts of risk and reward under conditions that are not completely rational. The most successful behavioral model of risky decision making is prospect theory (Kahneman and Tversky 1979b; Tversky and Kahneman 1992b). According to it, individuals make decisions based on the potential value of losses and gains among the set of available options. It proposes that individuals compute an internal evaluation for each prospect that is determined by a value function and a probability weighting function. The value function is S-shaped and asymmetrical, capturing loss aversion. The probability weighting function encodes the hypothesis that individuals overreact to small probability events, but under-react to large probability events. The theory deviates from its rational competitor, expected utility theory (Fishburn and Fishburn 1970), which assumes that people evaluate the outcome of a decision in terms of the expected reward, independent of any cognitive biases (such as risk aversion). Other recent theories explaining individual choices under risk/uncertainty include dynamic decision models (Pleskac, Diederich, and Wallsten 2015) such as dynamic field theory (Busemeyer and Townsend 1993).

### 3 Proposed Models of Decision Making

#### Decision Tasks

A team in our experiments consists of four humans and four AI agents. The accuracy of each AI agent is fixed during an experiment and ranges between 0.6 and 0.9. Humans are informed that the accuracy of each AI agent is at least 0.5. The reward for a correct answer  $c_1$  is 4, the penalty for an incorrect answer  $c_2$  is 1, and the penalty for consulting an AI agent  $c_3$  is 1. Multiple choice questions are posed sequentially to a team. After answering every five questions, each team member reports the relative influence of each member, which collectively generates a row stochastic weight matrix  $W$  (and the influence network) for the team. Each team member also rates the accuracy of the AI-agents after every five questions.

There are two sequential decision tasks in our experiment:

- **Decision Task 1. Integration of human responses and decision on the use of AI agents.** A team first needs to integrate the decisions of the team members into a group response, and decide whether it needs to utilize an AI agent to help answer the posed question correctly. And if an AI agent is to be invoked, the team needs to decide which of the four AI agents to use.
- **Decision Task 2. Integration of AI agent and human responses.** If an AI agent is consulted, then the team needs to integrate its response with the prior human responses into a group response.

Figure 1 shows the two decision tasks. The first decision task consists of eight possible actions: the first four actions  $A_{\theta_1}, \dots, A_{\theta_4}$  correspond to the decision of using one of the four choices to the posed question without consulting an agent, and the next four actions  $A_{g_1}, \dots, A_{g_4}$ , correspond to the decision of using an AI agent. Action  $A_{\theta_i}$  is associated with probability  $p_{\theta_i}$  while action  $A_{g_i}$  is associated with probability  $p_{g_i}$ . For the second decision task, the team needs to integrate the answer of an agent with the answers of the human team members and decide on one of the four choices. In this case, the task consists of four actions:  $A_{\theta_1}, \dots, A_{\theta_4}$ , which are associated with probabilities  $q_{\theta_1}, \dots, q_{\theta_4}$ , respectively. For a team to be successful, it needs to reach consensus on which action to take in the first decision task; furthermore, if one of the agents is chosen, then the team needs to achieve consensus on one of the four actions in the second decision task.

We next present a sequence of models that explain the decision making of a team. The first model uses Bayes rules to combine the individual choices into the team’s response. The second model achieves this integration through a weighting mechanism based on the eigenvector centralities of the individuals. The last two models utilize Prospect Theory to reflect how teams combine appraisal with decision making in risky environments.

#### Model NB: Integration through Bayes Rule

Model NB uses Bayes rule to integrate human-AI choices into a team response. We explain the model by considering first decision task depicted in Figure 1. The modeling can

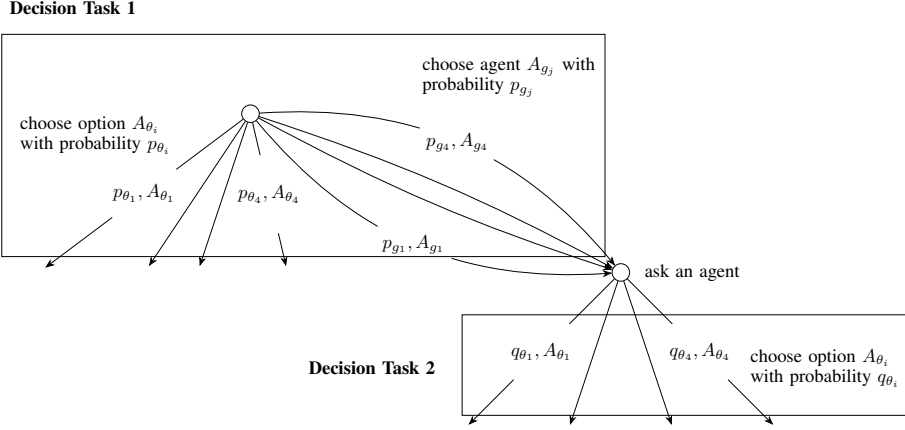


Figure 1: Decision making in the human-AI teams. The first decision task involves choosing one of the four options presented with each question or choosing one of the agents for help. The second decision task integrates the agent’s response with the earlier individual choices.

be broken down into three steps: Step 1 considers the individual responses made by individuals, Step 2 considers the choice of an agent, and Step 3 integrates the choices made in the previous two steps into a model for the eight actions in Figure 1.

**Step 1:** Let  $\Theta$  be the random variable corresponding to a team’s collective response. It ranges over the four choices to the posed question represented by  $\theta_i, i = 1 \dots 4$ . Let  $\theta^*$  be the correct choice. Let random variable  $R_i$  be the response of individual  $i$ . Model **NB** predicts the probability of the team reaching the decision on choice  $\theta_k$  as follows:

$$P(\Theta = \theta_k | R_i, i = 1 \dots 4) = \frac{P(R_i, i = 1 \dots 4 | \Theta = \theta_k) \times P(\Theta = \theta_k)}{P(R_i, i = 1 \dots 4)} \quad (1)$$

The above equation can be reduced by assuming that the individual choices are independent given the team’s choice:

$$p'_{\theta_k} = P(\Theta = \theta_k | R_i, i = 1 \dots 4) = \frac{(\prod_{i=1}^4 P(R_i | \Theta = \theta_k)) \times P(\Theta = \theta_k)}{P(R_i, i = 1 \dots 4)} \quad (2)$$

When  $R_i = \theta_k$ , the term  $P(R_i | \Theta = \theta_k)$  is assumed to equal  $E[\mathbf{1}\{R_i = \theta^*\}]$ , the expected performance of individual  $i$ . Otherwise,  $P(R_i | \Theta = \theta_k) = \frac{1 - E[\mathbf{1}\{R_i = \theta^*\}]}{3}$ . In other words, a team deciding the same as an individual’s choice assumes that the individual is correct and a team deciding differently from an individual assumes that the individual is incorrect. These assumptions imply that the group discovers the truth only if some individual suggests it. The value  $E[\mathbf{1}\{R_i = \theta^*\}]$  is defined by a beta distribution with two parameters that are initialized to one (leading to a uniform prior over the range  $[0,1]$ ), and updated after each response by an individual. The prior probabilities  $P(\Theta = \theta_k)$  are assumed to be 0.25, and the term in the denominator of Eq. 2 is found by normalization. Note that  $\mathbf{1}$  is the indicator function.

**Step 2:** The expected performance of agent  $i$  is again modeled using a beta distribution. The initial values of the two parameters are chosen so that we have a uniform prior over  $[0.5,1]$  to account for the fact that the accuracy of each agent is declared at the outset to be at least 0.5. The parameters are updated following each round in which an agent is consulted and its accuracy is observed. The probability of choosing agent  $g_i$  is  $p'_{g_i} = \frac{E[\mathbf{1}\{G_i = \theta^*\}]}{\sum_j E[\mathbf{1}\{G_i = \theta^*\}]}$ .

**Step 3:** Based on the probability of each action (choosing an option or an agent), we compute the expected reward for each possible action. The reward for choosing option  $\theta_i$  is  $x_{\theta_i} = c_1 \times p'_{\theta_i} - c_2 \times (1 - p'_{\theta_i})$ . And the reward for consulting agent  $i$  is  $x_{g_i} = (c_1 - c_3) \times p'_{g_i} - (c_2 + c_3) \times (1 - p'_{g_i})$ . We use the softmax function to transform  $x_{\theta_i}$  and  $x_{g_i}$  into probability values:

$$p_{\theta_i} = \frac{e^{x_{\theta_i}}}{\sum_j e^{x_{\theta_j}} + \sum_j e^{x_{g_j}}}, \quad (3)$$

$$p_{g_i} = \frac{e^{x_{g_i}}}{\sum_j e^{x_{\theta_j}} + \sum_j e^{x_{g_j}}}. \quad (4)$$

This concludes the modeling of the first decision task. Next, we consider how model **NB** explains the second decision task. Let  $g_j$  be the agent that the team consulted. We integrate the response  $G_j$  of the agent as follows:

$$q'_{\theta_k} = P(\Theta = \theta_k | R_i, i = 1 \dots 4, G_j) = \frac{(P(G_j | \Theta = \theta_k) \prod_{i=1}^4 P(R_i | \Theta = \theta_k)) \times P(\Theta = \theta_k)}{P(R_i, i = 1 \dots 4, G_j)} \quad (5)$$

When  $G_j = \theta_k$ , the term  $P(G_j | \Theta = \theta_k)$  is assumed to equal  $E[\mathbf{1}\{G_j = \theta^*\}]$ , the expected performance of agent  $j$ . Otherwise,  $P(G_j | \Theta = \theta_k) = \frac{1 - E[\mathbf{1}\{G_j = \theta^*\}]}{3}$ .  $P(R_i | \Theta = \theta_k)$  is defined similarly (and as in Eq. 2). Based on the above probabilities, we again compute the expected reward for each possible action. The reward for choosing option  $\theta_i$  is  $y_{\theta_i} = (c_1 - c_3) \times q'_{\theta_i} - (c_2 + c_3) \times (1 - q'_{\theta_i})$ . We again

use the softmax function to transform  $y_{\theta_i}$  into probability values:

$$q_{\theta_i} = \frac{e^{y_{\theta_i}}}{\sum_j e^{y_{\theta_j}}} \quad (6)$$

### Model CENT: Integration by Interpersonal Influence System

This model integrates individual responses through an interpersonal influence system. Each individual in the experiment is asked to rate the influence of other members in their team after every five questions. This leads to an influence network  $N$  (as shown in Figure 2) whose centralities are used to weigh the choices of the team members. Consider Decision Task 1 (Figure 1) first. The modeling is again done in three steps.

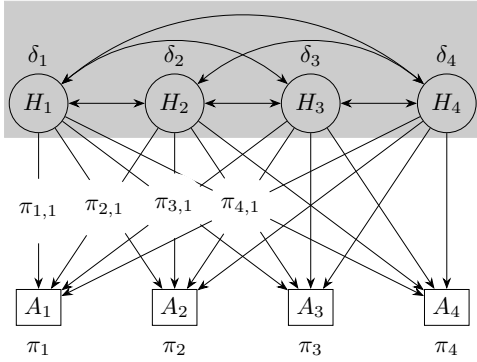


Figure 2: The appraisal networks. The shaded box is the appraisal matrix between the individuals on the team. The eigenvalues of the matrix are denoted by  $\delta$ . These individuals also appraise the agents. The  $\pi$  values denote these appraisals.

**Step 1:** The probability of the team choosing option  $\theta_k$  is modeled as the sum of the eigenvector centrality values in network  $N$  of each individual who has chosen option  $\theta_k$ . If the centrality value of individual  $i$  is  $\delta_i$  then we obtain the following for the probability of choosing option  $\theta_k$ .

$$p'_{\theta_k} = P(\Theta = \theta_k | R_i, i = 1 \dots 4) = \frac{\sum_i \mathbf{1}_{\theta_k}(R_i) \times \delta_i}{P(R_i, i = 1 \dots 4)} \quad (7)$$

**Step 2:** This step uses a weighting process to model the team's collective appraisal of the agents. Let the  $i$ -th individual's appraisal of the  $j$ -th agent be  $\pi_{ij}$ . Note that the values  $\pi_{ij}$  are collected during the experiment after every five questions. Let the eigenvector centrality values of individual  $i$  be  $\delta_i$  as before. We model the collective appraisal of agent  $j$  as  $\pi_j$  and the probability of choosing agent  $g_j$  as  $p'_{g_j}$ :

$$\pi_j = \sum_i \delta_i \pi_{ij} \quad (8)$$

$$p'_{g_j} = \frac{\pi_j}{\sum_j \pi_j} \quad (9)$$

**Step 3:** As in Step 3 of **NB**, we first compute the reward for each possible action and then transform all the rewards to probabilities using the softmax function.

This concludes the modeling of the first decision task. For the second decision task, we need to integrate the response  $G_j$  of the consulted agent  $j$  into the collective choice of the team. This integration now (as opposed to Decision Task 1) needs to consider the choice made by the agent and the choices made by the team prior to consultation with the agent. We utilize a parameter  $w$  for this integration:  $w$  weighs the influence placed in the agent's response as compared to the influence placed in the initial human responses. This (global) parameter is learned by a training sample of teams. We have the following resulting probability  $q'_{\theta_k}$  of choosing option  $\theta_k$  in Decision Task 2.

$$q'_{\theta_k} = P(\Theta = \theta_k | R_i, i = 1 \dots 4, G_j) = \frac{\mathbf{1}_{\theta_k}(G_j) \times \pi_j \times w + \sum_i \mathbf{1}_{\theta_k}(R_i) \times \delta_i \times (1 - w)}{P(R_i, i = 1 \dots 4, G_j)} \quad (10)$$

Based on these probabilities, we compute the expected rewards and derive the probabilities of choosing the four actions as in model **NB**.

### Model PT-NB: Integration through Prospect Theory and Naive Bayes

This model uses Prospect Theory to analyze the actions of the team as a set of gambles. For the first decision task, the estimation of probabilities  $p'_{\theta_i}, p'_{g_i}$  (Steps 1 and 2) is exactly as in model **NB**. Step 3 now utilizes Prospect Theory parameters to integrate them and obtain the probabilities for the eight actions.

We model the choices made by the team using five Prospect Theory parameters  $(\alpha, \beta, \lambda, \gamma^+, \gamma^-)$ .  $\alpha = \beta \in [0, 1]$ ,  $\gamma^{+/-} \in [0, 1]$ , and  $\lambda \in [0, 10]$ . The gamble for option  $\theta_i$  is  $\{(c_1, p'_{\theta_i}), (c_2, 1 - p'_{\theta_i})\}$  and the gamble for the use of agent  $g_i$  is  $\{(c_1 - c_3, p'_{g_i}), (c_2 + c_3, 1 - p'_{g_i})\}$ . The corresponding rewards  $x_{\theta_i}$  and  $x_{g_i}$  are computed as follows:

$$\begin{aligned} x_{\theta_i} &= c_1^\alpha \times \exp(-(\log \frac{1}{p'_{\theta_i}})^{\gamma^+}) \\ &\quad + \left( -\lambda |c_2|^\beta \times \exp(-(\log \frac{1}{1 - p'_{\theta_i}})^{\gamma^-}) \right) \\ x_{g_i} &= (c_1 - c_3)^\alpha \times \exp(-(\log \frac{1}{p'_{g_i}})^{\gamma^+}) \\ &\quad + \left( -\lambda |c_2 + c_3|^\beta \times \exp(-(\log \frac{1}{1 - p'_{g_i}})^{\gamma^-}) \right) \end{aligned} \quad (11)$$

Finally, we use the softmax function to transform these rewards into probability values  $p_{\theta_i}$  and  $p_{g_i}$ .

This concludes the modeling of the first decision task. The computations for the second decision task are similar. We use the probabilities  $q'_{\theta_k}$  from model **NB** and the Prospect Theory parameters to compute the rewards  $y_{\theta_i}$  and these are converted into probabilities  $q_{\theta_i}$  using the softmax function. Note that the gambles for all four options involve the same rewards and this will result in a similar model as **NB**.

### Model PT-CENT: Integration through Prospect Theory and Interpersonal Influence System

The development of this model is similar to **PT-NB** except that the model **CENT** is now used for computing the proba-

bilities  $p'_{\theta_i}$ ,  $p'_{g_i}$  and  $q'_{\theta_i}$ . Using the Prospect Theory parameters, we obtain the rewards  $x_{\theta_i}$ ,  $x_{g_i}$  and  $y_{\theta_i}$ . Finally, we use the softmax function to obtain the probabilities  $p_{\theta_i}$  and  $p_{g_i}$  for the eight actions in Decision Task 1 shown in Figure 1, and the probabilities  $q_{\theta_i}$  for the four actions in Decision Task 2 shown in Figure 1. Again, since the gambles for the four options involve the same rewards, this will result in a similar model as **CENT**.

## 4 Evaluation of Models

### Experimental Details

We worked with 30 teams, and 45 questions were sequentially posed to each team through the POGS (Kim et al. 2017) interface, a software system designed for conducting team experiments. Each intellectual question is coupled with four alternative answers. Each question is answered in four phases, of duration 30 seconds, 30 seconds, 15 seconds and 45 seconds, respectively. In the first phase, every team member records his/her initial individual response for the question. In the second phase, the responses of every team member are displayed on the screen and the chat plugin is enabled for communication. In the next 15 seconds, the team decides whether or not to invoke the help of an AI agent (and/or which AI agent to invoke); only one AI agent can be invoked per question. In the fourth phase, the team submits an answer. The correct answer to each question is displayed after submitting the answer. Over the sequence of 45 questions, this process generates an associated sequence of nine influence networks (denoted by a row-stochastic weight matrix  $W$ ). Consensus is reached by a team if each member chooses the same answer or chooses to invoke the same agent for help. If an agent is consulted then the team again needs to reach consensus on which answer to report. If consensus is not reached, then the task has failed and the team's response is deemed incorrect.

Our analysis is based on the  $9 \times 30 = 270$  occasions of team answers to the nine questions that involved a report of weight matrices. All the reported  $W$  are irreducible and aperiodic structures with a unique normalized left eigenvector, which we take as the measure of each team member's relative influence centrality. (These  $W$  matrices as well as the agent appraisal matrices  $\pi$  do converge in our experiments.) In turn, the measure of the influence centrality of a particular initial answer is the sum of the eigenvalues of those members who chose it as their initial (pre-discussion) answer. Thus, the influence's predicted answer for the team is the multiple choice alternative that has a largest sum of eigenvalue influence centralities.

### Results

Our main experimental results are about how well the proposed models predict decision making. In order to measure this correspondence, we first need to define a measurement criterion, or a loss function, that measures the correspondence between the model and the experimental data.

**Metrics for Measuring Model Accuracy** In both decision tasks, each of our models generates a probability distribution over the actions (eight actions in the first decision

task and four in the second). In the experimental data, we do not have the probability values the team computed, only the action chosen. As a result, we need to consider the distance between the model's predicted distribution and all possible data distributions in which the observed action is the dominant choice. We focus on measuring the smallest distance from a model to the family of possible distributions that fit the team's action. The other possibility of using an expected distance is considerably more complex since we need to assign probabilities to each feasible distribution. Let  $q$  be the specific distribution produced by a model with a maxima for action  $j$ , and let action  $i$  be the action chosen by the team. We consider all possible distributions  $p$  in which the value of  $p_i$  is as high as all  $p_k$ , and then compute the distance between the distributions to measure the correspondence. We adopt the measure of cross-entropy  $H$  for measuring the correspondence. Since cross-entropy is not symmetric, this gives us two possibilities. First, the loss function  $L^{(1)}$  minimizes the entropy  $H(q, p)$ :

$$L^{(1)} = \min_{p \text{ s.t. } \forall k: p_k \leq p_i} - \sum_{i=1}^n q_i \log(p_i) \quad (12)$$

(We have also considered the loss function  $L^{(2)}$  that minimizes  $H(p, q)$  with similar results.) Instead of generating all such distributions and finding the optimal  $p$ , we obtain an analytical solution. The distribution  $p$  that minimizes the loss function can be computed as follows:

$$\begin{aligned} i = j &\implies p = q \\ i \neq j &\implies p_k = \begin{cases} (1/n_H) \sum_{k \in q_H} q_k, & \text{if } k \in q_H \\ q_k, & \text{otherwise,} \end{cases} \end{aligned}$$

where  $q_H$  consists of those indices  $k$  for which  $q_k \geq q_i$  and  $n_H$  is the size of  $q_H$ .

**Random Baseline:** In order to assess the statistical significance of the models, we also compare with a baseline that makes a random choice uniformly among the possible actions at each step. For Decision Task 1, the probability of each action is 0.125 and for Decision Task 2, the probability of each action is 0.25.

**Learning Parameters** For models **PT-NB** and **PT-CENT** in the first decision task, we use the loss functions to learn the five parameters for Prospect Theory. We use a training set of 30 questions to learn these using grid search for each team. We vary the values of  $\alpha$ ,  $\beta$  and  $\gamma^{+/-}$  from 0 to 1 in steps of 0.1 and the value of  $\lambda$  from 0 to 10 in steps of 1. Using these parameters, we validate the models on the remaining 15 questions in the dataset for each team. For the second decision task, since the gambles for all four options involve the same rewards, models **PT-NB** and **PT-CENT** are similar to models **NB** and **CENT**, respectively. We only report the results of the latter two models. Parameter  $w$  in Equation 10 is learned by considering a random set of 20 teams and the results are validated on the remaining 10 teams.

**Validation of Models** For the first decision task in Figure 1, the loss values of each model are given in Table 1(a). As mentioned earlier, the values are averaged over 30

teams over the last 15 questions. The Wilcoxon signed-rank test (Wilcoxon 1992) shows the results of the four models are significantly superior to that of the random model (significance level  $< 0.01$ ). Table 1(b) shows that the appraisal-based models **NB** and **CENT** perform similarly in explaining a human-AI team’s decision making. The models **PT-NB** and **PT-CENT** also perform similarly and are superior to the previous two models (Wilcoxon signed-rank test significance level  $< 0.01$ ). This implies that modeling the inherent risk in decision making leads to a superior model.

Model	Loss $L^{(1)}$
<b>NB</b>	$1.08 \pm 0.16$
<b>CENT</b>	$1.14 \pm 0.14$
<b>PT-NB</b>	$0.55 \pm 0.19$
<b>PT-CENT</b>	$0.57 \pm 0.17$
<b>RANDOM</b>	$2.08 \pm 0$

(a)

Wilcoxon signed-rank test	$p$ -value for $L^{(1)}$
W( <b>NB</b> , <b>CENT</b> )	0.02
W( <b>NB</b> , <b>PT-NB</b> )	$< 0.01$
W( <b>NB</b> , <b>PT-CENT</b> )	$< 0.01$
W( <b>CENT</b> , <b>PT-NB</b> )	$< 0.01$
W( <b>CENT</b> , <b>PT-CENT</b> )	$< 0.01$
W( <b>PT-NB</b> , <b>PT-CENT</b> )	0.24

(b)

Table 1: (a) The loss values of (**NB**, **CENT**) are similar to each other and so are the loss values of (**PT-NB**, **PT-CENT**). The latter two models are superior suggesting that teams consider both risk/reward and appraisal in their decision making. (b) The models **PT-NB** and **PT-CENT** are significantly better than **NB** and **CENT**. (Wilcoxon signed-rank test. The null hypothesis is that the two related paired samples come from the same distribution.)

Next, we consider the second decision task in Figure 1. Since the risk/reward of each action is the same, models **PT-NB** and **NB** become similar, and so do models **PT-CENT** and **CENT**. Thus, we only report the values for **NB** and **CENT**. Since the AI agents are consulted about 25.7% of the time, there are fewer samples for this decision task. We learn the parameter  $w$  by considering a random set of 20 teams and present the validation results for the remaining 10 teams in Table 2(a). The parameter  $w$  is learned to be 0.9, suggesting that the teams consult the agents only when they are unsure of the choices and, as a result, and place a high degree of trust in the agent’s answer. Both models are superior to the random model (Wilcoxon signed-rank test significance level  $< 0.01$ ).

For the second decision task (when an AI agent is consulted), we also investigate how teams integrate the responses from the AI agents in their deliberations. For this, we designed two other models for this decision task: one in which the best human response is returned (neglecting the agent response) and another in which the agent’s response is returned (neglecting the human responses). Models **NB-H** and **CENT-H** are models of the former kind while **NB-A** and **CENT-A** are models of the latter kind. As can be seen from Table 2(a), models that rely only on human responses (**NB-H**

and **CENT-H**) do not explain the team behavior, suggesting that teams do integrate the agent responses. The good behavior of the agent-only models (**NB-A** and **CENT-A**) as well as the high value of parameter  $w$  (learned to be 0.9) suggests that teams rely much more on the agent response in this decision task. This can be explained by the fact that the teams proceed to the second decision task involving an AI agent only if they are unsure of the correct choice.

Model	Loss $L^{(1)}$
<b>NB</b>	$0.47 \pm 0.11$
<b>NB-H</b>	$0.91 \pm 0.20$
<b>NB-A</b>	$0.49 \pm 0.14$
<b>CENT</b>	$0.33 \pm 0.06$
<b>CENT-H</b>	$0.95 \pm 0.17$
<b>CENT-A</b>	$0.74 \pm 0.20$
<b>RANDOM</b>	$1.39 \pm 0$

(a)

Wilcoxon signed-rank test	$p$ -value for $L^{(1)}$
W( <b>NB</b> , <b>NB-A</b> )	0.02
W( <b>NB</b> , <b>NB-H</b> )	$< 0.01$
W( <b>NB-A</b> , <b>NB-H</b> )	$< 0.01$
W( <b>CENT</b> , <b>CENT-A</b> )	$< 0.01$
W( <b>CENT</b> , <b>CENT-H</b> )	$< 0.01$
W( <b>CENT-A</b> , <b>CENT-H</b> )	$< 0.01$

(b)

Table 2: (a) The models **NB** and **CENT** are the best at predicting the actions of a team. Models that rely on the human response only (**NB-H** and **CENT-H**) do not do as well, suggesting that the agent’s response is integrated into the final decision. Models that rely on the agent only (**NB-A** and **CENT-A**) also perform well, suggesting that the agent’s response is weighed highly in this decision task. (b) The models **NB** and **CENT** are significantly better than **NB-H** and **CENT-H**, respectively. Models **NB-A** and **CENT-A** are also significantly better than **NB-H** and **CENT-H**, respectively.

## 5 Conclusions

Our experimental setting provides a unique platform for understanding how human-AI team members learn each other’s expertise and how they coordinate to solve intellectual tasks in uncertain and risky environments. We proposed four models to explain the dynamics of human-AI team decision making. We find that, although appraisal-based models **NB** and **CENT** perform adequately in explaining human-AI team’s decision making, the prospect theory based models **PT-NB** and **PT-CENT** exhibit more accurate explanations. This finding establishes the importance of modeling the inherent risk in uncertain decision making. Our results raise a number of possibilities for future studies including the use of active AI participating agents and the use of reinforcement learning for modeling the decision making.

## References

Auer, P.; Cesa-Bianchi, N.; and Fischer, P. 2002. Finite-time analysis of the multiarmed bandit problem. *Machine Learning*, 47(2-3): 235–256.

- Baker, C.; Saxe, R.; and Tenenbaum, J. 2011. Bayesian Theory of Mind: Modeling Joint Belief-Desire Attribution. *Proceedings of the Thirty-Third Annual Conference of the Cognitive Science Society*.
- Bansal, G.; Nushi, B.; Kamar, E.; Lasecki, W.; Weld, D.; and Horvitz, E. 2019. Beyond Accuracy: The Role of Mental Models in Human-AI Team Performance. In *Proceedings of the AAAI Conference on Human Computation and Crowdsourcing*.
- Busemeyer, J. R.; and Townsend, J. T. 1993. Decision field theory: a dynamic-cognitive approach to decision making in an uncertain environment. *Psychological Review*, 100(3): 432–459.
- Cesa-Bianchi, N.; Freund, Y.; Haussler, D.; Helmbold, D. P.; Schapire, R. E.; and Warmuth, M. K. 1997. How to use expert advice. *Journal of the ACM*, 44(3): 427–485.
- Chaiken, S.; and Trope, Y., eds. 1999. *Dual-Process Theories in Social Psychology*. Guilford Press. ISBN 1572304219.
- Chen, J.; and Barnes, M. 2014. Human Agent Teaming for Multirobot Control: A Review of Human Factors Issues. *IEEE Transactions on Human-Machine Systems*, 44(1): 13–29.
- Crandall, J. W.; Oudah, M.; Ishowo-Oloko, F.; Abdallah, S.; Bonnefon, J.-F.; Cebrian, M.; Shariff, A.; Goodrich, M. A.; Rahwan, I.; et al. 2018. Cooperating with machines. *Nature communications*, 9(1): 233.
- Cummings, M. 2014. Man versus Machine or Man + Machine? *IEEE Intelligent Systems*, 29(5): 62–69.
- Cuzzolin, F.; Morelli, A.; Cîrstea, B.; and Sahakian, B. J. 2020. Knowing me, knowing you: theory of mind in AI. *Psychological Medicine*, 50(7): 1057–1061.
- DeCostanza, A.; Marathe, A.; Bohannon, A.; Evans, A.; Palazzolo, E.; Metcalfe, J.; and McDowell, K. 2018. Enhancing Human-Agent Teaming with Individualized, Adaptive Technologies: A Discussion of Critical Scientific Questions. US Army Research Laboratory Technical Report.
- DeGroot, M. H. 1974. Reaching a consensus. *Journal of the American Statistical Association*, 69(345): 118–121.
- Der Kiureghian, A.; and Ditlevsen, O. 2009. Aleatory or epistemic? Does it matter? *Structural Safety*, 31(2): 105–112.
- Endsley, M. R.; and Kaber, D. B. 1999. Level of automation effects on performance, situation awareness and workload in a dynamic control task. *Ergonomics*, 42(3): 462–492.
- Fishburn, P. C.; and Fishburn, C. S. 1970. *Utility Theory for Decision Making*. Operations Research Society of America. Publications in operations research. Wiley. ISBN 9780471260608.
- Fox, C. R.; and Ülkümen, G. 2011. Distinguishing two dimensions of uncertainty. In Brun, W.; Keren, G.; Kirkebøen, G.; and Montgomery, H., eds., *Perspectives on Thinking, Judging and Decision-Making*. Universitetsforlaget. ISBN 978-8215018782.
- French, J.; Raven, B.; and Cartwright, D. 1959. The bases of social power. *Classics of organization theory*, 7: 311–320.
- Friedkin, N. E.; and Johnsen, E. C. 2011. *Social Influence Network Theory: A Sociological Examination of Small Group Dynamics*. Cambridge University Press. ISBN 9781107002463.
- Friedkin, N. E.; Mei, W.; Proskurnikov, A. V.; and Bullo, F. 2019. Mathematical Structures in Group Decision-Making on Resource Allocation Distributions. *Scientific Reports*, 9(1): 1377.
- Garcia, J. O.; Brooks, J.; Kerick, S.; Johnson, T.; Mullen, T. R.; and Vettel, J. M. 2017. Estimating direction in brain-behavior interactions: Proactive and reactive brain states in driving. *Neuroimage*, 150: 239–249.
- Gaur, Y.; Lasecki, W. S.; Metze, F.; and Bigham, J. P. 2016. The effects of automatic speech recognition quality on human transcription latency. In *Proceedings of the 13th Web for All Conference*, 23. ACM.
- Kahneman, D.; and Tversky, A. 1979a. Prospect theory: An analysis of decision under risk. *Econometrica*, 47(2): 363–391.
- Kahneman, D.; and Tversky, A. 1979b. Prospect theory: An analysis of decision under risk. *Econometrica*, 47(2): 363–391.
- Kamar, E.; Hacker, S.; and Horvitz, E. 2012. Combining human and machine intelligence in large-scale crowdsourcing. In *Proceedings of the 11th International Conference on Autonomous Agents and Multiagent Systems-Volume 1*, 467–474. International Foundation for Autonomous Agents and Multiagent Systems.
- Kim, Y. J.; Engel, D.; Woolley, A. W.; Lin, J. Y.-T.; McArthur, N.; and Malone, T. W. 2017. What makes a strong team?: Using collective intelligence to predict team performance in League of Legends. In *Proceedings of the 2017 ACM Conference on Computer Supported Cooperative Work and Social Computing*, 2316–2329. ACM.
- Li, S.; Sun, W.; and Miller, T. 2016. Communication in Human-Agent Teams for Tasks with Joint Action. In Dignum, V.; Noriega, P.; Sensoy, M.; and Sichman, J. S., eds., *Coordination, Organizations, Institutions, and Norms in Agent Systems XI*, 224–241. Springer.
- Marathe, A. R.; Metcalfe, J. S.; Lance, B. J.; Lukos, J. R.; Jangraw, D.; Lai, K.-T.; Touryan, J.; Stump, E.; Sadler, B. M.; Nothwang, W.; and McDowell, K. 2018a. The privileged sensing framework: A principled approach to improved human-autonomy integration. *Theoretical Issues in Ergonomics Science*, 19(3): 283–320.
- Marathe, A. R.; Schaefer, K. E.; Evans, A. W.; and Metcalfe, J. S. 2018b. Bidirectional Communication for Effective Human-Agent Teaming. In Chen, J. Y. C.; and Fragomeni, G., eds., *Virtual, Augmented and Mixed Reality: Interaction, Navigation, Visualization, Embodiment, and Simulation*, 338–350. Springer.
- Mei, W.; Friedkin, N. E.; Lewis, K.; and Bullo, F. 2017. Dynamic models of appraisal networks explaining collective learning. *IEEE Transactions on Automatic Control*, 63(9): 2898–2912.



Nilsson, H.; Rieskamp, J.; and Wagenmakers, E.-J. 2011. Hierarchical Bayesian parameter estimation for cumulative prospect theory. *Journal of Mathematical Psychology*, 55(1): 84–93.

Oguntola, I.; Hughes, D.; and Sycara, K. P. 2021. Deep Interpretable Models of Theory of Mind For Human-Agent Teaming. *CoRR*, abs/2104.02938.

O’Neill, T.; McNeese, N.; Barron, A.; and Schelble, B. 2020. Human-Autonomy Teaming: A Review and Analysis of the Empirical Literature. *Hum Factors*.

Pleskac, T. J.; Diederich, A.; and Wallsten, T. S. 2015. Models of decision making under risk and uncertainty. In Busemeyer, J. R.; Wang, Z.; Townsend, J. T.; and Eidels, A., eds., *The Oxford handbook of computational and mathematical psychology*, 209–231. New York: Oxford University Press.

Premack, D.; and Woodruff, G. 1978. Does the chimpanzee have a theory of mind? *Behavioral and Brain Sciences*, 1(4): 515–526.

Rabinowitz, N.; Perbet, F.; Song, F.; Zhang, C.; Eslami, S. A.; and Botvinick, M. 2018. Machine Theory of Mind. In *International Conference on Machine Learning*, 4215–4224.

Rasmussen, J. 1987. Skills, Rules, and Knowledge; Signals, Signs, and Symbols, and Other Distinctions in Human Performance Models. *IEEE Transactions on Systems, Man and Cybernetics*, 13: 257–266.

Schapire, R. E. 1990. The strength of weak learnability. *Machine Learning*, 5(2): 197–227.

Sheridan, T. B.; and Verplank, W. L. 1978. Human and computer control of undersea teleoperators. Technical report, MIT, Man-Machine Laboratory, Cambridge, MA.

Shirado, H.; and Christakis, N. A. 2017. Locally noisy autonomous agents improve global human coordination in network experiments. *Nature*, 545(7654): 370.

Simon, H. A. 1957. *Models of Man: Social and Rational*. Mathematical Essays on Rational Human Behavior in a Social Setting. Wiley.

Stubbs, K.; Hinds, P. J.; and Wettergreen, D. 2007. Autonomy and common ground in human-robot interaction: A field study. *IEEE Intelligent Systems*, 22(2).

Telesford, Q. K.; Lynall, M. E.; Vettel, J.; Miller, M. B.; Grafton, S. T.; and Bassett, D. S. 2016. Detection of functional brain network reconfiguration during task-driven cognitive states. *Neuroimage*, 142: 198–210.

Tversky, A.; and Kahneman, D. 1992a. Advances in prospect theory: Cumulative representation of uncertainty. *Journal of Risk and uncertainty*, 5(4): 297–323.

Tversky, A.; and Kahneman, D. 1992b. Advances in prospect theory: Cumulative representation of uncertainty. *Journal of Risk and Uncertainty*, 5(4): 297–323.

Wang, D.; Khosla, A.; Gargaya, R.; Irshad, H.; and Beck, A. H. 2016. Deep learning for identifying metastatic breast cancer. *arXiv preprint arXiv:1606.05718*.

Wegner, D. M. 1987. Transactive memory: A contemporary analysis of the group mind. In Mullen, B.; and Goethals, G. R., eds., *Theories of Group Behavior*, 185–208. Springer.

Welinder, P.; Branson, S.; Perona, P.; and Belongie, S. J. 2010. The multidimensional wisdom of crowds. In *Advances in Neural Information Processing Systems*.

Wilcoxon, F. 1992. Individual comparisons by ranking methods. In *Breakthroughs in statistics*, 196–202. Springer.

Woolley, A. W.; Chabris, C. F.; Pentland, A.; Hasnmi, N.; and Malone, T. W. 2010. Evidence for a Collective Intelligence Factor in the Performance of Human Groups. *Science*, 330: 686–688.

## A Background

### Appraisal Dynamics

Individuals in a team appraise their own and others’ displayed positions on issues. These appraisals may be based on individuals’ task-relevant information, expertise, friendships, authority, or charisma (French, Raven, and Cartwright 1959). A team’s level task-performance depends on how these bases condition the allocation of relative influence to themselves and others ( $0 \leq w_{ij} \leq 1 \forall i, \sum_{j=1}^n w_{ij} = 1 \forall i$ ). The set of these weights defines a row-stochastic matrix  $W$ . This matrix is associated with an influence network  $\mathcal{G}$  composed of  $i \xrightarrow{w_{ij} > 0} j$  arcs of  $i$ ’s accorded relative direct influence to  $j$ . We assume that team’s members’ positions evolve according to (DeGroot 1974)

$$X(k+1) = WX(k) = \dots = W^k X(0), \quad k = 1, 2, \dots,$$

where  $X(0)$  represents the initial choices. If an initial consensus exists, then the prediction is that it will be maintained. If initial disagreement exists, then the existence of at least one globally reachable individual in  $\mathcal{G}$  is a sufficient condition for the convergence of the influence system to consensus. A team with one globally reachable individual in  $\mathcal{G}$  will form a consensus on the initial position of that individual. A team in which all individuals are mutually reachable in  $\mathcal{G}$  will form a compromise consensus if  $W$  is irreducible with at least one  $0 < w_{ii} < 1$ . In all of the above cases, the convergence to consensus is associated with a unique normalized left eigenvector of  $W$  in which each eigenvalue is the total (direct and indirect) relative influence centrality of an individual’s initial position on the team’s consensus. Over a sequence of issues, the  $W$  that is constructed by a team may differ from issue to issue, and along with such modifications the individuals’ influence centralities may also vary over the issue sequence.

### Prospect Theory

In human decision making, the classic method of eliciting risk preference behavior is to present a sequence of choice dilemmas. A subject is presented with a series of problems and asked to select their preferred *mixed gamble* in the set  $\{X = ((x_1, p_1), (x_2, p_2)), Y = ((y_1, q_1), (y_2, q_2))\}$ , where  $x_1, y_1 \geq 0$  are \$-valued gains and  $x_2, y_2 < 0$  are \$-valued losses. Selecting gamble  $X$  results in a payment of  $\$x_1$  with probability  $p_1$  or a debt of  $\$x_2$  with probability  $p_2$ . Similarly for  $Y$ . Cumulative Prospect Theory proposes that individuals maintain an internal valuation function  $V(X)$  assigning

a psychological value to a set of risky outcomes called a prospect. The valuation function  $V(X)$  for mixed gamble  $X$  decomposes as

$$V(X) = v^+(x_1)w^+(p_1) + v^-(x_2)w^-(p_2), \quad (13)$$

where the value function  $v^{+/-}(\cdot)$  and weighting function  $w^{+/-}(\cdot)$  depend on the perception of the outcome relative to a reference point (i.e., is the outcome a gain or loss of capital, social status, etc.).

Prospect theory defines a set of parameters  $\theta = (\alpha, \beta, \lambda, \gamma^+, \gamma^-)$ , with the following natural interpretation (Nilsson, Rieskamp, and Wagenmakers 2011):  $\alpha$  (resp.  $\beta$ ) denotes sensitivity to gain (resp. loss) outcomes,  $\lambda$  denotes perceived impact of loss relative to gain,  $\gamma^+$  (resp.  $\gamma^-$ ) denotes the degree to which gain (loss) probabilities are over- or under-weighted. Thus, the value function  $v^{+/-}(\cdot)$  and weighting function  $w^{+/-}(\cdot)$  are defined as follows:

$$\begin{aligned} v^+(x) &= x^\alpha, & \alpha > 0, \\ v^-(x) &= -\lambda|x|^\beta, & \lambda, \beta > 0, \\ w^+(p) &= \exp\left(-\left(\log \frac{1}{p}\right)^{\gamma^+}\right), & \gamma^+ > 0, \\ w^-(p) &= \exp\left(-\left(\log \frac{1}{p}\right)^{\gamma^-}\right), & \gamma^- > 0. \end{aligned} \quad (14)$$

## B Alternative Loss Functions

The main body of the paper considered a metric  $L^{(1)}$  for measuring the accuracy of models. Here, we consider two other possible metrics (or loss functions). The first is  $L^{(2)}$ , the symmetric counterpart to  $L^{(1)}$ .

$$L^{(2)} = \min_{p \text{ s.t. } \forall k: p_k \leq p_i} - \sum_{i=1}^n p_i \log(q_i) \quad (15)$$

We obtain an analytical solution to the above optimization problem as follows. Let  $q_j$  be a maximum value in  $q$ . The distribution  $p$  that minimizes the above loss function can be computed as follows (Theorem C.5 in the appendix).

- $p = q$ , if  $i = j$
- Otherwise,

$$p_k = (1/n), k \in q_H \\ = 0, \text{ otherwise}$$

where  $q_H$  consists of those indices  $k$  for which  $q_k \geq q_i$ ,  $n$  is the size of  $q_H$ .

We also consider binary loss  $L^{(b)}$ :

$$L^{(b)} = - \sum_{i=1}^n p_i \log(q_i) \quad (16)$$

where  $p_i = 1$  if the team choose the  $i$ -th action, otherwise  $p_i = 0$ .

It should be noted that the  $L^{(2)}$  loss values for the **PT-NB** and **PT-CENT** models do not decrease in the same manner as that for  $L^{(1)}$  loss values. This can be explained by considering how the second loss function is minimized. If the set  $q_H$  (Eq. 15) does not change then the value of  $L^{(2)}$  also does

not change (we find that  $q_H$  does not change between the non-PT and PT-based models in about half of the test cases). On the other hand,  $L^{(1)}$  is more sensitive and it can change even if the set  $q_H$  does not change. Tables 3 and 4 show the loss values corresponding to  $L^{(b)}$  and  $L^{(2)}$  for the four models and their significance comparisons in the first decision task, respectively. The orderings of the values in the two tables are roughly similar to those in Tables 1 and 2 presented earlier.

Model	Loss $L^{(b)}$	Loss $L^{(2)}$
<b>NB</b>	$1.28 \pm 0.41$	$1.22 \pm 0.21$
<b>CENT</b>	$1.17 \pm 0.34$	$1.19 \pm 0.18$
<b>PT-NB</b>	$1.16 \pm 0.30$	$1.10 \pm 0.29$
<b>PT-CENT</b>	$1.11 \pm 0.33$	$1.00 \pm 0.31$
<b>RANDOM</b>	$2.08 \pm 0$	$2.08 \pm 0$

Table 3: Loss values of the models in the first decision task.

Wilcoxon signed-rank test	$L^{(b)}$	$L^{(2)}$
<b>W(NB,CENT)</b>	<0.01	0.12
<b>W(NB,PT-NB)</b>	<0.01	<0.01
<b>W(NB,PT-CENT)</b>	<0.01	<0.01
<b>W(CENT,PT-NB)</b>	0.72	<0.01
<b>W(CENT,PT-CENT)</b>	0.01	<0.01
<b>W(PT-NB, PT-CENT)</b>	0.17	<0.01

Table 4: Significance level ( $p$ -value) of the Wilcoxon signed-rank test for models in Decision Task 1. The null hypothesis is that the two related paired samples come from the same distribution.

Table 5 shows the loss values corresponding to  $L^{(b)}$  and  $L^{(2)}$  for the models **NB**, **NB-H**, **NB-A**, **CENT**, **CENT-H**, and **CENT-A** in the second decision task. Table 6 shows the corresponding significance comparisons. The orderings of values in the two tables again reflect that in Tables 3 and 4, suggesting robustness of the results.

Model	Loss $L^{(b)}$	Loss $L^{(2)}$
<b>NB</b>	$0.50 \pm 0.27$	$0.54 \pm 0.16$
<b>NB-H</b>	$1.43 \pm 0.37$	$1.15 \pm 0.29$
<b>NB-A</b>	$0.64 \pm 0.47$	$0.71 \pm 0.33$
<b>CENT</b>	$0.59 \pm 0.46$	$0.48 \pm 0.20$
<b>CENT-H</b>	$1.24 \pm 0.41$	$1.09 \pm 0.26$
<b>CENT-A</b>	$0.67 \pm 0.39$	$0.84 \pm 0.27$
<b>RANDOM</b>	$1.39 \pm 0$	$1.39 \pm 0$

Table 5: Loss values of models in the second decision task.

Wilcoxon signed-rank test	$L^{(b)}$	$L^{(2)}$
<b>W(NB,NB-A)</b>	0.51	<0.01
<b>W(NB,NB-H)</b>	<0.01	<0.01
<b>W(NB-A,NB-H)</b>	0.02	<0.01
<b>W(CENT,CENT-A)</b>	0.51	<0.01
<b>W(CENT,CENT-H)</b>	0.04	<0.01
<b>W(CENT-A,CENT-H)</b>	0.06	<0.01

Table 6: Significance level ( $p$ -value) of the Wilcoxon signed-rank test for models in Decision Task 2. The null hypothesis is that the two related paired samples come from the same distribution.

## C Proofs of Lemmas and Theorems

**Lemma C.1.** For any  $0 \leq x_1 \leq x_2 \leq 1$  and  $0 \leq y_2 \leq y_1 \leq 1$ ,

$$-(y_1 \log x_1 + y_2 \log x_2) \geq -(y_1 + y_2) \log \frac{x_1 + x_2}{2}$$

*Proof.* Since the function  $\log(x)$  is concave,

$$\begin{aligned} \log \frac{x_1 + x_2}{2} &\geq \frac{1}{2} \log x_1 + \frac{1}{2} \log x_2 \\ (y_1 + y_2) \log \frac{x_1 + x_2}{2} &\geq \frac{y_1 + y_2}{2} \log x_1 + \frac{y_1 + y_2}{2} \log x_2 \\ &= y_1 \log x_1 + y_2 \log x_2 + \frac{y_2 - y_1}{2} \log x_1 + \frac{y_1 - y_2}{2} \log x_2 \\ &= y_1 \log x_1 + y_2 \log x_2 + \frac{y_2 - y_1}{2} (\log x_1 - \log x_2) \\ &= y_1 \log x_1 + y_2 \log x_2 + \frac{y_2 - y_1}{2} \log \frac{x_1}{x_2} \\ &\geq y_1 \log x_1 + y_2 \log x_2 \end{aligned}$$

□

The following lemma gives us an optimal solution to  $\min_q H(p, q)$  over all distributions with mass  $m_q$ .

**Lemma C.2.** Given a distribution  $q$  with a total mass  $m_q = \sum_i q_i$ , among all distributions with a mass of  $m_p$ , the distribution that minimizes  $-\sum_i q_i \log p_i$ , is  $p^* = \frac{m_p}{m_q} q$ .

*Proof.* Consider any  $p$  with  $m_p = \sum_i p_i$ .

$$\begin{aligned} -\sum_i p_i \log q_i &= -\sum_i p_i \log \frac{q_i}{m_q} - \sum_i p_i \log m_q \\ &= -m_p \sum_i \frac{p_i}{m_p} \log \frac{q_i}{m_q} - m_p \log m_q \\ &= m_p H\left(\frac{p}{m_p}, \frac{q}{m_q}\right) - m_p \log m_q \\ &\geq m_p H\left(\frac{p}{m_p}\right) - m_p \log m_q \end{aligned}$$

Since  $p^* = \frac{m_p}{m_q} p$ , it follows that

$$\begin{aligned} -\sum_i p_i \log q_i^* &= m_p H\left(\frac{p}{m_p}, \frac{q^*}{m_q}\right) - m_p \log m_q \\ &= m_p H\left(\frac{p}{m_p}, \frac{p}{m_p}\right) - m_p \log m_q \\ &= m_p H\left(\frac{p}{m_p}\right) - m_p \log m_q \end{aligned}$$

Therefore,  $-\sum_i p_i \log q_i \geq -\sum_i p_i \log q_i^*$ . □

The above two lemmas imply that given a probability distribution  $q$ , in order to construct a distribution  $p$  whose maximum value is constrained to be at  $i$  and whose cross-entropy  $H(q, p)$  is minimized with respect to  $q$ , values in  $p$  must be chosen such that  $p_i = p_j = \eta$  if  $q_i \leq q_j$ , and the remaining mass is distributed over  $p$  according to the shape of  $q$ . The following theorem establishes the optimal  $p$  based on these considerations.

**Theorem C.3.** Given a distribution  $q$ , a distribution  $p$  with a maxima at  $i$  that minimizes the cross-entropy  $H(q, p)$  is defined as follows:

$$\begin{aligned} p_k &= \eta \text{ if } k \in q_H, \\ &= q_k, \text{ otherwise} \end{aligned}$$

where  $q_H$  consists of those indices  $k$  for which  $q_k \geq q_i$ ,  $n$  is the size of  $q_H$ , and  $\eta = \frac{\sum_{k \in q_H} q_k}{n}$ .

*Proof.* From Lemma C.1,  $p_i = p_k = \alpha, k \in q_H$  for optimal  $H(q, p)$ . Furthermore, from Lemma C.2, for optimal  $H(q, p)$ , for any  $k \notin q_H$ ,  $p_k = (1 - n\alpha) \frac{q_k}{m}$ , where  $m = \sum_{l \notin q_H} q_l$ . Thus, at any optimal  $p$ ,

$$\begin{aligned} H(q, p) &= -\left(\sum_{k \in q_H} q_k\right) \log \alpha - \sum_{k \notin q_H} q_k \log \left((1 - n\alpha) \frac{q_k}{m}\right) \\ \frac{dH(q, p)}{d\alpha} &= -\frac{\sum_{k \in q_H} q_k}{\alpha} + \frac{n \sum_{k \notin q_H} q_k}{1 - n\alpha} \\ &= -\frac{\sum_{k \in q_H} q_k}{\alpha} + \frac{nm}{1 - n\alpha} \\ &= \frac{n\alpha(m + \sum_{k \in q_H} q_k) - \sum_{k \in q_H} q_k}{\alpha(1 - n\alpha)} \\ &= \frac{n\alpha - \sum_{k \in q_H} q_k}{\alpha(1 - n\alpha)} \end{aligned}$$

Note that at any feasible solution,  $0 < \alpha \leq \frac{1}{n}$ . The above derivative is negative when  $\alpha < \eta$  and positive when  $\alpha > \eta$ . Furthermore, when  $\alpha = \eta$ ,  $p_k = q_k < \eta, \forall k \notin q_H$ . Therefore,  $\alpha = \eta$  is a feasible solution. □

**Lemma C.4.** For any  $0 \leq x_1 \leq x_2 \leq 1$  and  $0 \leq y_2 \leq y_1 \leq 1$ ,

$$-(x_1 \log y_1 + x_2 \log y_2) \geq -\left(\frac{x_1 + x_2}{2} \log y_1 + \frac{x_1 + x_2}{2} \log y_2\right)$$

*Proof.*

$$\begin{aligned}
& - (x_1 \log y_1 + x_2 \log y_2) + \left( \frac{x_1 + x_2}{2} \log y_1 + \frac{x_1 + x_2}{2} \log y_2 \right) \\
&= \frac{x_2 - x_1}{2} \log y_1 - \frac{x_2 - x_1}{2} \log y_2 \\
&= \frac{x_2 - x_1}{2} (\log y_1 - \log y_2) \geq 0
\end{aligned}$$

□

**Theorem C.5.** *Given a distribution  $q$ , a distribution  $p$  with a maxima at  $i$  that minimizes the cross-entropy  $H(p, q)$  is defined as follows:*

$$\begin{aligned}
p_k &= (1/n) \text{ if } k \in q_H, \\
&= 0, \text{ otherwise}
\end{aligned}$$

where  $q_H$  consists of those indices  $k$  for which  $q_k \geq q_i$ ,  $n$  is the size of  $q_H$ .

*Proof.* Combining our constraints  $p_i \geq p_k$  with Lemma C.4 implies that at optimal  $p$ ,  $p_i = p_k$ ,  $k \in q_H$ . Next, we analyze which of the remaining entries in  $p$  should be non-zero. Consider when a transfer of mass  $\alpha$  from  $\{p_k\}_{k \in q_H}$  to  $p_l$ ,  $l \notin q_H$ , reduces the entropy  $H(p, q)$ . For this, we must have

$$\begin{aligned}
-\alpha \log q_l &< -\left( \sum_{k \in q_H} (\alpha/n) \log q_k \right) \\
-\log q_l &< -\frac{1}{n} \sum_{k \in q_H} \log q_k
\end{aligned}$$

Since  $q_k > q_l$ ,  $k \in q_H$ ,  $l \notin q_H$ , this statement is always false. Hence, all of the mass of  $p$  will concentrate on  $q_H$  and be uniformly distributed. Since there are  $n$  elements of  $q_H$ , then  $p_k = (1/n)$ ,  $\forall k \in q_H$  is an optimal solution.

□